Critical interpretation of CH– and OH– stretching regions for infrared spectra of methanol clusters (CH3OH) n (n = 2–5) using self-consistent-charge density functional tight-binding molecular dynamics simulations

Yoshifumi Nishimura, Yuan-Pern Lee, Stephan Irle, and Henryk A. Witek

Citation: The Journal of Chemical Physics **141**, 094303 (2014); doi: 10.1063/1.4893952
View online: http://dx.doi.org/10.1063/1.4893952
View Table of Contents: http://scitation.aip.org/content/aip/journal/jcp/141/9?ver=pdfcov
Published by the AIP Publishing

Articles you may be interested in

Methanol clusters (CH3OH) n , n = 3–6 in external electric fields: Density functional theory approach
J. Chem. Phys. **135**, 024307 (2011); 10.1063/1.3605630

Finite-temperature infrared spectroscopy of polycyclic aromatic hydrocarbon molecules. II. Principal mode analysis and self-consistent phonons
J. Chem. Phys. **133**, 074303 (2010); 10.1063/1.3465554

Structures of water- CO 2 and methanol- CO 2 cluster ions: [H 2 O • (CO 2) n] + and [CH 3 OH • (CO 2) n] + (n = 1 – 7)
J. Chem. Phys. **130**, 154304 (2009); 10.1063/1.3116144

The vibrational spectra of protonated water clusters: A benchmark for self-consistent-charge density-functional tight binding
J. Chem. Phys. **127**, 234504 (2007); 10.1063/1.2806992

IR + vacuum ultraviolet (118 nm) nonresonant ionization spectroscopy of methanol monomers and clusters: Neutral cluster distribution and size-specific detection of the OH stretch vibrations
J. Chem. Phys. **124**, 024302 (2006); 10.1063/1.2141951

This article is copyrighted as indicated in the article. Reuse of AIP content is subject to the terms at: http://scitation.aip.org/termsconditions. Downloaded to IP: 140.113.38.11 On: Thu, 25 Dec 2014 01:20:11

Critical interpretation of CH– and OH– stretching regions for infrared spectra of methanol clusters $(CH_3OH)_n$ ($n = 2$–5) using self-consistent-charge density functional tight-binding molecular dynamics simulations

Yoshifumi Nishimura,[1,2] Yuan-Pern Lee,[2,3] Stephan Irle,[1,4] and Henryk A. Witek[2,a)]
[1]*Department of Chemistry, Nagoya University, Furo-cho, Chikusa-ku, Nagoya 464-8602, Japan*
[2]*Department of Applied Chemistry and Institute of Molecular Science, National Chiao Tung University, 1001 Ta-Hsueh Road, Hsinchu 30010, Taiwan*
[3]*Institute of Atomic and Molecular Sciences, Academia Sinica, P.O. Box 23-166, Taipei 10617, Taiwan*
[4]*Institute of Transformative Bio-Molecules (WPI-ITbM), Nagoya University, Furo-cho, Chikusa-ku, Nagoya 464-8602, Japan*

(Received 7 June 2014; accepted 13 August 2014; published online 2 September 2014)

Vibrational infrared (IR) spectra of gas-phase O–H···O methanol clusters up to pentamer are simulated using self-consistent-charge density functional tight-binding method using two distinct methodologies: standard normal mode analysis and Fourier transform of the dipole time-correlation function. The twofold simulations aim at the direct critical assignment of the C–H stretching region of the recently recorded experimental spectra [H.-L. Han, C. Camacho, H. A. Witek, and Y.-P. Lee, J. Chem. Phys. **134**, 144309 (2011)]. Both approaches confirm the previous assignment (*ibid.*) of the C–H stretching bands based on the B3LYP/ANO1 harmonic frequencies, showing that ν_3, ν_9, and ν_2 C–H stretching modes of the proton-accepting (PA) and proton-donating (PD) methanol monomers experience only small splittings upon the cluster formation. This finding is in sharp discord with the assignment based on anharmonic B3LYP/VPT2/ANO1 vibrational frequencies (*ibid.*), suggesting that some procedural faults, likely related to the breakdown of the perturbational vibrational treatment, led the anharmonic calculations astray. The IR spectra based on the Fourier transform of the dipole time-correlation function include new, previously unaccounted for physical factors such as non-zero temperature of the system and large amplitude motions of the clusters. The elevation of temperature results in a considerable non-homogeneous broadening of the observed IR signals, while the presence of large-amplitude motions (methyl group rotations and PA-PD flipping), somewhat surprisingly, does not introduce any new features in the spectrum. © *2014 AIP Publishing LLC*. [http://dx.doi.org/10.1063/1.4893952]

I. INTRODUCTION

Vibrational spectroscopy is frequently employed to characterize chemical structures of complex systems.[1,2] Infrared (IR) and Raman spectra of biological samples, condensed phase systems, and large polyatomic molecules possess in general quite complex character due to the overlap of multiple spectral signals, including overtones and combination bands, which make straightforward interpretation of experimental results a difficult, cumbersome, and partially speculative task. To assist the analysis, theoretical modeling of IR and Raman spectra plays nowadays a very important role. The standard computational approach is based on the so-called normal mode analysis (NMA),[1] in which harmonic vibrational frequencies of a system are determined by diagonalization of the mass-weighted Hessian matrix at the equilibrium molecular geometry. The associated IR and Raman intensities are then computed from the rotational invariants of the first derivatives of molecular dipole moment ($\boldsymbol{\mu}$) and molecular polarizability ($\boldsymbol{\alpha}$), respectively, (i.e., the norm of $\boldsymbol{\mu}$ and the trace and anisotropy of $\boldsymbol{\alpha}$) along the corresponding vibrational modes.[1,3,4] This approach, usually referred to as the double harmonic approximation, is subject to a number of systematic errors, causing deviation from experimentally measured vibrational spectra: (i) the calculated harmonic vibrational frequencies are typically too high with respect to experiment, (ii) the coupling between vibrational modes is neglected, (iii) overtones and combination bands are not reproduced, (iv) resonances are not included, and (v) band intensities are poorly represented, to name only a few. In order to compensate partially for these effects, various *a posteriori* techniques are usually employed. The simplest of these is an *ad hoc* fix that brings the computed frequencies toward those observed in experiment by applying empirical scaling factors;[5] their dependence on the level of theory and on the basis set has been extensively discussed.[6–11] An alternative approach takes the effect of coupling between harmonic normal modes into account in vibrational state calculations, where the required potential energy surface around equilibrium structure is expanded with higher order terms[12,13] or represented utilizing pair-wise interactions.[14] Unfortunately, heavy computational cost prevents one from applying this approach to

a)Author to whom correspondence should be addressed. Electronic mail: hwitek@mail.nctu.edu.tw

 © 2014 AIP Publishing LLC

This article is copyrighted as indicated in the article. Reuse of AIP content is subject to the terms at: http://scitation.aip.org/termsconditions. Downloaded to IP: 140.113.38.11 On: Thu, 25 Dec 2014 01:20:11

large molecular systems. Another drawback shared by the two approaches discussed above concerns two very fundamental differences between the experimental and theoretical systems. Namely, the experiment is always conducted on an *ensemble of molecules* at some *finite* temperature, while theoretical simulations almost always concern a *single molecule or molecular clusters* at $T = 0$ K. Needless to say, the last two fundamental differences between experimental vibrational spectra and those derived by NMA as mentioned above may lead to very different character of the measured and simulated spectra, especially with regards to the intensity patterns.

A powerful alternative to NMA is extracting IR and Raman spectra from molecular dynamics (MD) simulations using the Fourier transformation of appropriate time correlation functions (FT-TCF).[15–17] The usual methodology of obtaining the FT-TCF spectra is quite simple. First, a MD trajectory for a given molecular ensemble at some finite temperature is simulated and a sequence of values of $\boldsymbol{\mu}$ (for IR spectra) and/or of $\boldsymbol{\alpha}$ (for Raman spectra) is recorded as a function of time. Subsequently, the spectrum is constructed from the Fourier transform of the time autocorrelation functions of $\boldsymbol{\mu}$ or $\boldsymbol{\alpha}$. In principle, it is sufficient to perform the Fourier transformation on data obtained from a single MD trajectory, but for practical purposes this approach is not advisable as the trajectory should be exceedingly long in order to allow the ensemble to visit all important sampling region of the configuration phase space. Instead, it is much more practical to assume the validity of the ergodic hypothesis, run a large number of independent MD trajectories, and average the resulting partial spectra into the final vibrational IR or Raman spectra. Note that the quality of spectra obtained in this way seems to confirm the validity of this hypothesis. It seems sufficient to average approximately 100 partial spectra, but in exceptional cases this number can be larger before the convergence of sampling is achieved. FT-TCF spectra naturally account for the anharmonic and finite-temperature effects can appropriately address bulk materials, and enable one to estimate the positions and intensities of overtones and/or combination bands. The advantages are slightly overshadowed by limitations associated with a large number of expensive MD trajectories required, which limits the applicability of this approach to relatively small systems.[18–23] Another difficulty associated with this approach concerns the somewhat cumbersome way of assigning the observed spectral bands to particular molecular vibrations.[24–27]

In the current study, to overcome the computational time limitations, we employ the self-consistent-charge density functional tight-binding (SCC-DFTB or shortly DFTB) method.[28,29] DFTB can be regarded as an approximated version of density functional theory (DFT).[30,31] The approximations allow for considerable time savings in comparison to DFT and permit one to treat systems containing up to a few thousands of atoms and to run MD trajectories as long as a few nano-seconds with accuracy comparable but slightly inferior to DFT. The resulting finite temperature, dynamic vibrational FT-TCF/DFTB spectra, used previously in a number of studies,[32–39] can be compared with the usual NMA/DFTB spectra, which are readily computable using the analytical SCC-DFTB Hessian code[40–42] and have been reported in a number of publications.[43–47] Note that the benchmark calculations suggest that SCC-DFTB is more accurate than other semi-empirical methods for vibrational analysis,[48] especially when used in conjunction with the parameters re-optimized especially for this purpose.[49]

In the current study, we employ the FT-TCF/DFTB formalism for modeling the IR spectra of methanol clusters. Methanol is one of the simplest organic molecules having a capability to form hydrogen-bonded clusters. The mechanism responsible for the cluster formation is similar to that involved in the formation of water clusters, but new phenomena, such as hydrophobic interactions of methyl groups or participation of the C–H bonds in weak hydrogen bonding, can also play some role. Theoretical predictions of stable forms of methanol clusters, their binding energies, and vibrational spectra are highly desirable to assist further understanding of these systems. In experiment, an usual source of information about methanol clusters is gas-phase IR spectroscopy.[50–55] Computational studies of such clusters typically rely on DFT or *ab initio* methods.[56–69] In recent years, special attention was given to comprehend the spectral fingerprint of methanol clusters in the C–H stretching and the O–H stretching regions as the function of the number of monomers.[50–54,70] In particular, our recent publication[54] reported a joint experimental-computational study of the IR absorption spectra of gas-phase $(CH_3OH)_n$ clusters with $n = 2$–6 in the spectral region 2650–3750 cm^{-1}. The spectra corresponding to larger clusters ($n = 3$–6) were quite similar to each other, suggesting common, cyclic structure of these aggregates. The spectra attributed to $(CH_3OH)_2$ were apparently different and suggested that one of the methanol molecules serves as a proton donor (PD) and the other, as a proton acceptor (PA). The spectra displayed a number of sharp features (at 3675, 3576, 3006, 2984, 2955, 2934, 2849, and 2823 cm^{-1}), which could be assigned as the O–H (ν_1) or C–H (ν_2, ν_3, and ν_9) stretching vibrations of PA and PD. To assign the observed bands to particular vibrational modes, NMA analysis was performed at the B3LYP/ANO1 level of theory,[54] which suggested that the spectrum of $(CH_3OH)_2$ can be easily derived from the IR spectrum of a single methanol molecule, in which the modes corresponding to PA are slightly shifted toward higher frequencies, while the modes corresponding to PD experience considerably larger shift toward lower frequencies. This picture agreed well with chemical intuition anticipated for such a donor-acceptor complex. The calculated PA–PD harmonic splittings of the ν_3, ν_9, and ν_2 modes (36, 53, and 35 cm^{-1}, respectively) compared favorably with experimentally observed splittings (26, 21, and 22 cm^{-1}, respectively), but the predicted positions of bands were too high. The perturbative inclusion of anharmonic effects, resulting in the B3LYP/VPT2/ANO1 scheme,[54,71,72] predicted the positions of the bands more accurately but completely revolutionized the assignment of experimentally observed spectral signals (for details, see Figure 1), giving an interwoven pattern with much larger splittings (126, 59, and 40 cm^{-1}, respectively).

The sharp discord between the assignments based on the harmonic and VPT2 anharmonic frequencies discussed above indicates that anharmonicity may constitute an important factor in interpretation of experimental vibrational spectra of

This article is copyrighted as indicated in the article. Reuse of AIP content is subject to the terms at: http://scitation.aip.org/termsconditions. Downloaded to IP: 140.113.38.11 On: Thu, 25 Dec 2014 01:20:11

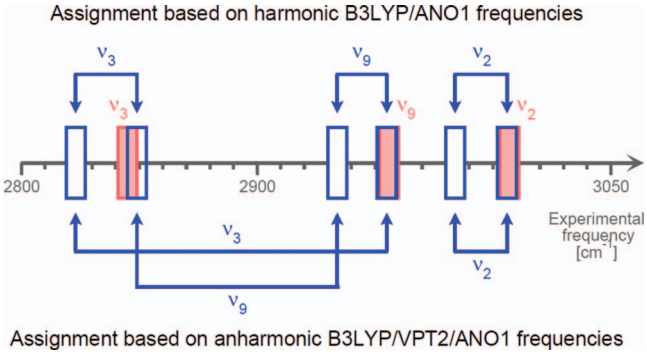

FIG. 1. Experimental[54] vibrational frequencies of the C–H stretching modes for methanol dimer (blue rectangles) and methanol monomer (red rectangles). Theoretical mode assignments based on harmonic B3LYP/ANO1 (top) and anharmonic B3LYP/VPT2/ANO1 (bottom) frequencies[54] are in sharp discord.

weakly bound molecular clusters. This finding may have serious consequences as vast majority of assignments of the recorded experimental spectra is still based on the scaled harmonic frequencies. It would not be surprising if the above discussed sharp difference between the harmonic and VPT2 anharmonic interpretations for the $(CH_3OH)_2$ cluster is not limited only to this particular system. In the worst case, our finding may signify that a critical re-evaluation of all the assignments of vibrational spectra of weakly bound systems that were based on simulated harmonic frequencies is required. This would constitute a considerable computational effort with possibly far-reaching implications that may revolutionize our knowledge about weakly bound clusters. Therefore, it is highly desirable to verify first with some alternative approach whether the previous anharmonic frequency analysis based on the B3LYP/VPT2/ANO1 scheme was correct. To this end, we employ in the current study the SCC-DFTB method to calculate the harmonic (NMA based) and non-harmonic (FT-TCF based at three low temperatures up to 100 K) IR spectra for CH_3OH clusters consisting of two to five methanol molecules. The results obtained with these two methodologies seem to confirm each other and show the same interpretations as the one based on harmonic frequencies (B3LYP/ANO1) in spite of the presence of large-amplitude motions (methyl group rotations and PA-PD flipping) in molecular dynamics trajectories. This, in turn, suggests that the anharmonic vibrational frequencies[54] computed with vibrational perturbation theory[71,72] based on B3LYP potential energy surfaces may carry significant computational errors and can lead to serious interpretational artifacts. Reasons for such behavior are most likely associated with the break-down of the vibrational perturbation theory; solutions to these problems remain to be investigated.

The structure of the current study is as follows. Section II gives the details of our computational approach. The presentation of results in Sec. III starts with a validation of the employed SCC-DFTB methodology by comparing the energetics and structural parameters of the optimized low-energy isomers of methanol clusters with *ab initio* and DFT. Subsequently, we present the simulated FT-TCF spectra of methanol clusters and compare them with experimental data and with the standard harmonic IR spectra obtained using the NMA/DFTB approach. The assignment of the FT-TCF spectra is then presented using the time-correlation functions of the symmetrized internal coordinates. Finally, we study the effect of temperature on the simulated spectra and give the most important conclusions of our study in Sec. IV.

II. COMPUTATIONAL DETAILS

Geometries of methanol clusters (M_n, $n = 2$–5) were optimized at the SCC-DFTB level of theory employing standard *mio* parameter sets[29] and standard thresholds for force (10^{-5} a.u.) and charge (10^{-12} a.u.) convergence criteria. The SCC-DFTB equilibrium structures were then used to perform SCC-DFTB, B3LYP,[73,74] and second-order Møller-Plesset perturbation theory (MP2)[75] single-point energy calculations with 6-311+G(d,p) basis set[76,77] in order to evaluate cluster binding energies and to determine relative stability of conceivable isomers using Gaussian 09 suite of programs.[78] Counterpoise corrections were taken into consideration for B3LYP and MP2 to compensate the basis set superposition error (BSSE).[79]

The NMA/DFTB harmonic IR spectra were simulated from calculated vibrational frequencies and intensities under the assumption that each vibrational band can be represented as a Gaussian with a half-width of 2.5 cm^{-1}. For reference, the BLYP/6-311+G(d,p)[74,76,77,80] vibrational analysis was carried out. No scaling of the harmonic frequencies was attempted to allow meaningful comparisons with the computed FT-TCF/DFTB vibrational IR spectra at low temperature. IR intensities are represented in arbitrary units.

The FT-TCF/DFTB vibrational IR spectra were generated using the following procedure. In the first step, canonical ensemble (NVT) MD simulations were performed to reach the desired temperature starting from the energetically most stable cluster. This heating process was run for 2.5 ps by means of the Berendsen thermostat.[81] The target temperatures T were set to $T = 10$, 50, and 100 K. Higher temperature MD simulations led to the dissociation of clusters. Note that in experiment no equipartition of energy is expected for the vibrational and rotational degrees of freedom; the clusters are expected to be rotationally quite cold (about 10 K), while vibrational temperature can be much higher (possibly up to 150 K or even 250 K). This effect has not been included in our simulations. Next, dipole moment components computed from Mulliken atomic charges and Cartesian coordinates were collected at each time step during 50 ps microcanonical ensemble (NVE) MD simulations. For both NVT and NVE simulations, the modified version of TINKER program package[82,83] interfaced with the SCC-DFTB code was used. The integration scheme of Newton's equations of motion was based on the Beeman algorithm[84,85] and the chosen time step was 0.5 fs. We run 100 independent trajectories per model systems to ensure the convergence of the intensity pattern. Fourier transform of dipole autocorrelation function with a Blackman filter[86] to minimize the noise was calculated for the last 2^{16} (=65 536) data points of each trajectory consisting of 10^5 MD steps using the FFTW3 library.[87] Both the length of data sampling and the time step are responsible for the frequency resolution in the obtained power spectrum. The

This article is copyrighted as indicated in the article. Reuse of AIP content is subject to the terms at: http://scitation.aip.org/termsconditions. Downloaded to IP: 140.113.38.11 On: Thu, 25 Dec 2014 01:20:11

employed conditions suggest a resolution of about 1 cm^{-1}, which is sufficient for the purpose of the current study. The theoretical IR adsorption intensity $A(\omega)$[88] for the vibrational mode with frequency ω is given by

$$A(\omega) = \frac{\hbar\beta\omega^2}{2\pi}\int_{-\infty}^{\infty}\langle\mu(0)\cdot\mu(t)\rangle\exp(-i\omega t)dt, \qquad (1)$$

where $\hbar$ is the reduced Planck's constant, β is inverse of Boltzmann constant k_b multiplied by temperature ($\beta = 1/k_bT$), and the dipole moment autocorrelation function is denoted as $\langle\mu(0)\cdot\mu(t)\rangle$.

III. RESULTS AND DISCUSSION

A. SCC-DFTB performance assessment for methanol clusters

Figure 2 displays the structures of methanol clusters considered in this study. The list of the presented structures does not pretend to be complete. Methanol can form assorted types of clusters via the O–H···O hydrogen bonding, leading to an enormous number of isomers for a large value of n. We have selected the cyclic polygon structures shown in Figure 2 since earlier publications[57,59,62,64–68] reported that these clusters are energetically preferable over open chains or cyclic rings with branched structure. Each selected isomer is classified using the labels "u" and "d" (denoting the "up" or "down" orientation of methyl groups with respect to the approximately planar ring formed by the oxygen atoms) following the definition in Ref. 66.

The optimized SCC-DFTB geometries are similar to those computed with B3LYP/6-31G(d). The SCC-DFTB hydrogen bonds become slightly longer (0.03–0.07 Å) than for B3LYP as the size of clusters increases. Similar discrepancy is observed in water clusters[89,90] even though the dispersion term[91] was included. Elstner suggests that the effect originates from the underestimation of Pauli repulsion within the minimal basis set.[92] It is important to note that both B3LYP and SCC-DFTB predict a decrease in the hydrogen bonding distances and an elongation of the O–H bonds with the growing size of the cluster. These tendencies can be perceived as a

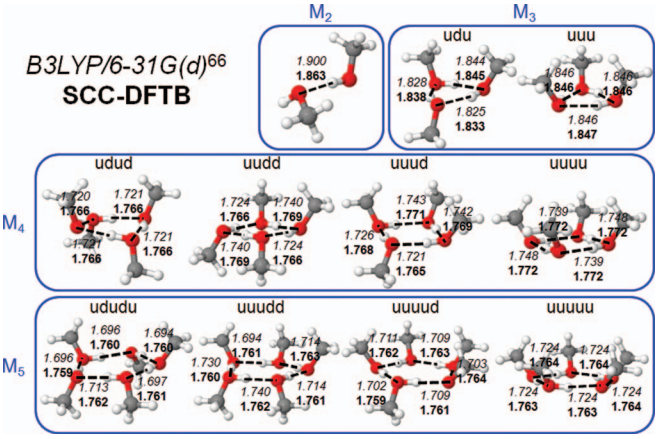

FIG. 2. Optimized SCC-DFTB and B3LYP/6-31G(d) intermolecular bond lengths (Å) in methanol clusters M_n, $n = 2$–5. The B3LYP results taken from Ref. 66 when available; otherwise recomputed. The labels u and d are defined in text.

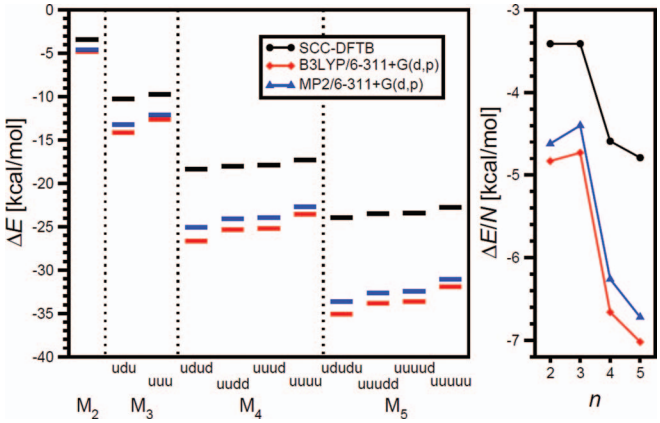

FIG. 3. Left panel: Intermolecular interaction energies ΔE (kcal/mol) of methanol clusters M_n, $n = 2$–5 at the SCC-DFTB geometries. BSSE corrections are included except for the SCC-DFTB results. Right panel: ΔE of the most stable isomers divided by the number of formed hydrogen bonds N.

cooperative effect.[60,61,64] The SCC-DFTB O–H bond lengths are 0.992 Å (PD) and 0.981 Å (PA) for dimer, 0.998 Å for trimer, 1.003 Å for tetramer and pentamer, irrespective of the conformer.

The left panel of Figure 3 shows intermolecular interaction energies $\Delta E = E(M_n) - n \times E(M_1)$ computed at the SCC-DFTB equilibrium geometry for each conformer with $n = 2$–5 with SCC-DFTB, B3LYP, and MP2 where M_1 stands for methanol monomer. Zero-point energy and thermal corrections were not considered. The computed $|\Delta E|$ increases with n. The strength of a hydrogen bond has been roughly estimated by dividing ΔE by the number N of hydrogen bonds in the cluster. The right panel of Figure 3 presents $\Delta E/N$ for dimer, "udu" trimer, "ududu" tetramer, and "ududu" pentamer. Both MP2 and B3LYP methods have produced similar interaction energies. The MP2 method accounts for dynamical electron correlation effects and naturally includes dispersion interactions. On the other hand, B3LYP fails to describe weak interactions adequately[93,94] while it works well for relatively strong hydrogen bonded interactions.[95–97] Small differences between MP2 and B3LYP suggest that the O–H···O intermolecular hydrogen bonding is responsible for the dominant part of ΔE. The underestimation of hydrogen bonded interactions at the SCC-DFTB level has already been pointed out in the study of binding energies for water clusters.[92,98–102] It is noteworthy that recent extension of SCC-DFTB method by introducing third order term and damped electron-electron interaction function (i.e., DFTB3) improves hydrogen bonding properties.[101,103,104]

To summarize the observations in the current section, the SCC-DFTB method provides us with a correct qualitative description of geometric and energetic properties of methanol clusters, which makes us confident while proceeding to the MD simulations of the IR spectra.

B. SCC-DFTB harmonic and anharmonic IR spectra of methanol clusters

Before entering into details, it is indispensable to discuss the convergence of IR spectral shape obtained from the FT-TCF simulations. Figure 4 shows the convergence of the

This article is copyrighted as indicated in the article. Reuse of AIP content is subject to the terms at: http://scitation.aip.org/termsconditions. Downloaded to IP: 140.113.38.11 On: Thu, 25 Dec 2014 01:20:11

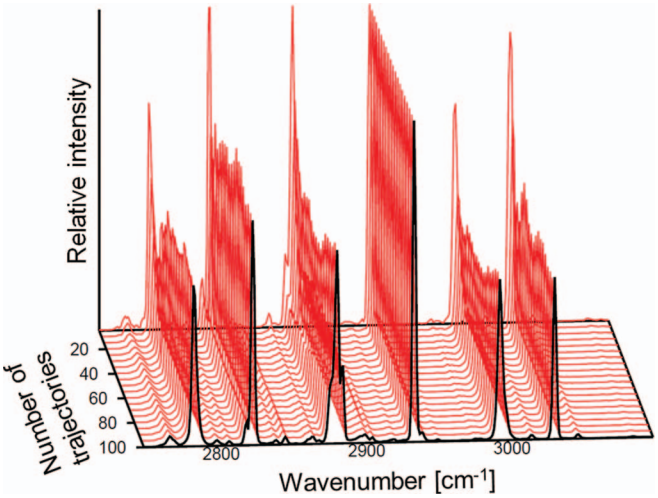

FIG. 4. Evolution of simulated FT-TCF/DFTB IR spectra with respect to the number of averaged MD trajectories for methanol dimer M_2 at $T = 10$ K.

simulated spectra in the C–H stretching region with the number of averaged MD trajectories for the methanol dimer M_2 at $T = 10$ K. Relative IR intensities show some fluctuations when a small number of trajectories have been averaged. These undesired features are gradually reduced when the number of trajectories is increased. The data presented in the subsequent sections of this manuscript are obtained by averaging spectra from 100 trajectories, which seem to be a fair compromise from the perspective of reliability and computational demands. Unless otherwise noted, all FT-TCF/DFTB vibrational IR spectra have been always produced that way.

The simulated harmonic NMA spectra of methanol clusters are presented in Figure 5. The spectra have been simulated for the most stable isomer of each cluster with NMA/DFTB and compared with the NMA/BLYP results. For the C–H stretching region, the BLYP and DFTB intensity patterns are similar. Quantitatively—but not qualitatively—the simulated NMA/DFTB and NMA/BLYP spectra are quite similar; the number of peaks, their relative intensity patterns, their division into subfamilies, vibrational echoes, etc., seem to agree quite well. Both families of spectra show quite close

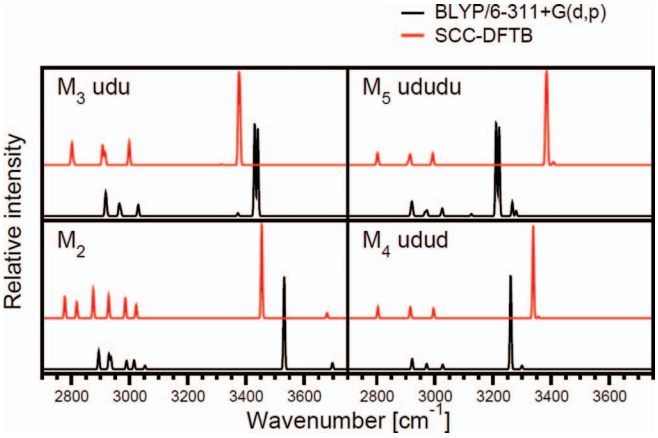

FIG. 5. Harmonic IR spectra of methanol clusters M_n, $n = 2$–5 computed with NMA/BLYP/6-311+G(d,p) (black) and NMA/DFTB (red).

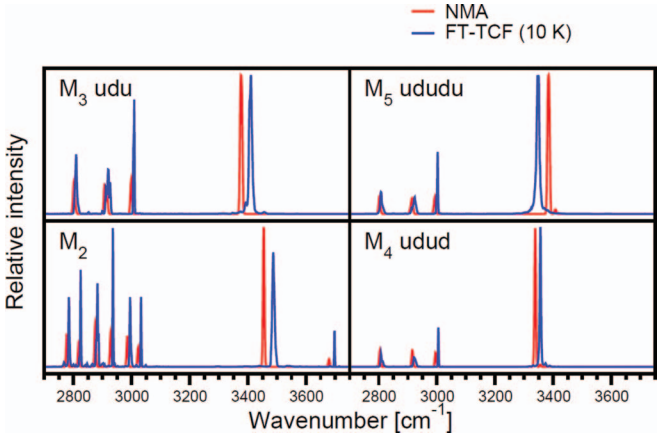

FIG. 6. IR spectra of methanol clusters M_n, $n = 2$–5 computed with SCC-DFTB using NMA (red) and FT-TCF (blue) methodologies.

resemblance to experimental data[54] but it is difficult to state unequivocally that NMA/BLYP is superior to NMA/DFTB or vice versa. Largest discrepancies between the DFTB and BLYP spectra can be as large as 100 cm^{-1}. While such large discrepancies between the two methods may seem quite substantial if one wants to validate experimental assignments, we would like to point out that our focus here is on the comparison between spectra computed within the same method, i.e., DFTB, but using two different frameworks, NMA and FT-TCF, in order to elucidate the effects of anharmonicity and finite temperature on the interpretation of the methanol dimer IR spectra.

The vibrational IR spectra of methanol clusters obtained with FT-TCF/DFTB at $T = 10$ K are shown in Figure 6 together with the harmonic NMA/DFTB results. We have rarely observed any transformation between isomers during the MD simulations at $T = 10$ K. Note that several cases of interesting behavior such as methyl group rotation and switching the role of PD and PA in the dimer have been found at higher temperatures, but openings of the rings formed by the O–H···O hydrogen bonds in our MD trajectories have never been detected. The choice of such a low temperature seems to be proper for straightforward comparisons between NMA and FT-TCF. These two sets of spectra seem to be quite similar. The main difference between them concerns primarily altered positions of O–H peaks in the FT-TCF spectra, which are usually elevated by some 10–30 cm^{-1} with respect to NMA. This behavior is most likely a manifestation of strong anharmonicities in the O–H stretching mode. The C–H stretching region is similar for both sets of spectra except for considerable transfer of intensity between the O–H and C–H stretch regions and slightly altered intensity pattern in the group of bands associated with the C–H stretching modes. The altered intensity patterns can be understood in terms of band broadening associated with large anharmonic character of some vibrations. Note that bands which appear smaller in the FT-TCF spectra are usually much broader than in the corresponding NMA spectra.

Qualitative understanding of the FT-TCF/DFTB spectra obtained at $T = 10$ K allows us to proceed to the analysis of analogous spectra recorded at higher temperatures, which

This article is copyrighted as indicated in the article. Reuse of AIP content is subject to the terms at: http://scitation.aip.org/termsconditions. Downloaded to IP: 140.113.38.11 On: Thu, 25 Dec 2014 01:20:11

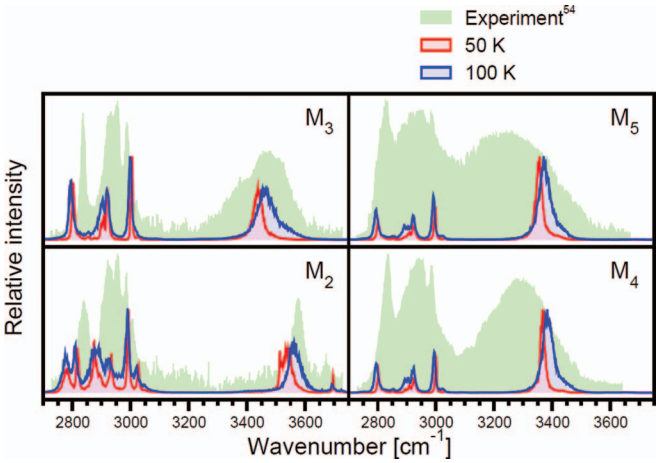

FIG. 7. IR spectra of methanol clusters M_n, $n = 2$–5 simulated at $T = 50$ K (red) and $T = 100$ K (blue) with FT-TCF/DFTB. The corresponding experimental[54] spectra are depicted as green shadowed background.

correspond more realistically to the experimental situation we want to model. For this purpose, we have performed simulations of the FT-TCF/DFTB spectra at $T = 50$ K and at $T = 100$ K. These spectra are presented in Figure 7. It is clear that higher temperature alters the character of the FT-TCF/DFTB spectra significantly broadening and merging the otherwise distinct IR bands; the broadening is proportional to the increase in temperature. The positions of the bands in the C–H region are only slightly influenced by temperature but the position of the band associated with the O–H stretch undergoes significant blueshift at higher temperatures. Note that the experimental spectra[54] for the M_2–M_5 clusters—presented as the green shadow background in each graph of Figure 7—show quite good agreement with our simulations, even if the substantially broader character of the bands suggests that vibrational temperature in experiment can be considerably higher than 100 K. (Estimation of experimental temperature in our case is a highly speculative task; it seems realistic to imagine that the rotational and translational temperature of the observed clusters is as low as 5–20 K, while the vibrational temperature can be as high as 150–250 K.) Clearly, it would be beneficial to obtain the FT-TCF spectra corresponding to higher temperatures but, as mentioned earlier, DFTB simulations at higher temperatures (e.g., the molecular trajectory of M_3 at 200 K) often result in a dissociation of the clusters.

Our main objective in the current work is to reinvestigate the interpretation of the C–H fingerprint region in the experimental IR spectrum of the methanol dimer. For this purpose, we need to introduce a method for assigning the vibrational bands in the FT-TCF/DFTB spectrum. Such a technique is discussed in Sec. III C.

C. Characterization of FT-TCF/DFTB bands

One of the main difficulties of the FT-TCF formalism is the interpretation of bands and their assignment to particular vibrational modes. Various techniques have been designed in the past to address this issue.[24–27,105–112] Martinez *et al.* proposed a method for decomposing calculated vibrational spectra as a sum of effective normal mode contributions extracted from the Fourier transform of velocity autocorrelation functions data.[24] Aiming at more appropriate treatment for large floppy molecules, that concept was extended by describing localized vibrational modes as linear combinations of non-redundant internal coordinates.[25] Other choices are to execute a series of instantaneous normal mode analysis (INMA)[105,106] for structural snapshots[26,27,107,108] or to perform principal mode analysis.[107,109–111]

Our strategy for characterization of the simulated FT-TCF bands consists of a number of steps. (i) First, the Cartesian coordinates of methanol clusters M_2 are collected during each NVE MD simulation. (ii) The collected Cartesian coordinates are projected onto the symmetrized[113] internal coordinates of each methanol monomer—defined graphically in Table I—resulting in a time-dependent amplitude $\nu_N(t)$ for each internal mode. Note that the information about translations, rotations, and intermolecular vibrations is lost in this process. Note also that the sets of indistinguishable atoms must be treated appropriately in order to obtain meaningful results; details are discussed in Sec. III D devoted to large-amplitude motions in the methanol dimer. (iii) Power spectra for each vibrational mode ν_N is obtained via FT of the autocorrelation function[114–118] $\langle \nu_N(0) \cdot \nu_N(t) \rangle$ for 100

TABLE I. Symmetrized[113] internal coordinates of methanol ν_N, $N = 1$–12. Figure in the right panel defines atomic labels, bonds, and angles.

N	ν_N	Comments
1	r_{OH}	OH stretch
2	$(2r_1 - r_2 - r_3)/\sqrt{6}$	CH d-stretch
3	$(r_1 + r_2 + r_3)/\sqrt{3}$	CH s-stretch
4	$(2\alpha_1 - \alpha_2 - \alpha_3)/\sqrt{6}$	CH_3 d-deformation
5	$(\beta_1 + \beta_2 + \beta_3 - \alpha_1 - \alpha_2 - \alpha_3)/\sqrt{6}$	CH_3 s-deformation
6	β_4	OH bend
7	$(2\beta_1 - \beta_2 - \beta_3)/\sqrt{6}$	CH_3 rock
8	r_{CO}	CO stretch
9	$(r_2 - r_3)/\sqrt{2}$	CH d-stretch
10	$(\alpha_2 - \alpha_3)/\sqrt{2}$	CH_3 d-deformation
11	$(\beta_2 - \beta_3)/\sqrt{2}$	CH_3 rock
12	τ	H^1COH torsion

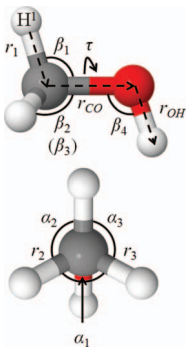

This article is copyrighted as indicated in the article. Reuse of AIP content is subject to the terms at: http://scitation.aip.org/termsconditions. Downloaded to IP: 140.113.38.11 On: Thu, 25 Dec 2014 01:20:11

independent trajectories; the resulting power spectra are subsequently superposed. (iv) Peak positions in FT of the $\langle \nu_N(0) \cdot \nu_N(t) \rangle$ power spectra coincide with the positions of peaks in FT of $\langle \mu(0) \cdot \mu(t) \rangle$; relative height of a peak observed at some frequency ω_i corresponds to the contribution from a given internal coordinate ν_N to the vibrational activity of the whole molecule occurring with the frequency ω_i. The results of such analysis for the C–H stretching modes of the methanol dimer M_2 at $T = 10$ K are presented in the upper panel of Figure 8 together with the previously discussed FT-TCF spectra of IR adsorption. It is clear that the vibrational frequencies obtained from the analysis of an oscillating dipole moment and from the analysis of oscillating internal coordinates coincide. The six prominent IR peaks in the C–H stretching region can be almost uniquely assigned to vibrational modes of the two methanol molecules—PD and PA—forming the methanol dimer M_2. The IR bands at 2936 and 2883 cm^{-1} correspond to the ν_9 vibrational mode of PA and PD, respectively. The IR bands at 3032 and 2995 cm^{-1} correspond predominantly (90%) to the ν_2 vibrational mode of PA and PD, respectively, with a small admixture (<8%) of the intramolecular ν_3 vibrational mode. Similarly, the IR bands at 2825 and 2784 cm^{-1} correspond predominantly (90%) to the ν_3 vibrational mode of PA and PD, respectively, with a small admixture (<10%) of the intramolecular ν_2 vibrational mode. More detailed data on the decomposition of each IR band into the ν_2, ν_3, and ν_9 modes of PA and PD are given in Table II. Note that this decomposition data can be treated as an analog for the standard potential energy distribution analysis performed often for the NMA spectra.[119–124] The assignment in the upper panel of Figure 8 confirms almost perfectly the assignment from Figure 1 based on harmonic NMA/DFTB and B3LYP vibrational frequencies at low temperature molecular dynamics simulations as expected the similarity of spectral patterns in Figure 6.

Elevation of temperature from 10 K to 50 K does not introduce any major changes in the interpretation of the bands in the IR spectra of methanol dimer discussed above. The FT-TCF/DFTB power spectra obtained at 10 K and 50 K differ primarily by their band widths (for the ν_3 mode of PA, it is 3 cm^{-1} at 10 K and 9 cm^{-1} at 50 K) and slightly altered pattern of mode mixing (the admixture of ν_2 to the ν_3 vibrational mode of PA is 8.9% at 10 K and 4.6% at 50 K). Further elevation of temperature from 50 K to 100 K does not change this picture much. The bands undergo further widening but their positions and character are altered only in a small degree. The FT-TCF/DFTB spectra obtained at 50 K naturally include the effect of methyl group rotation and the spectra obtained at

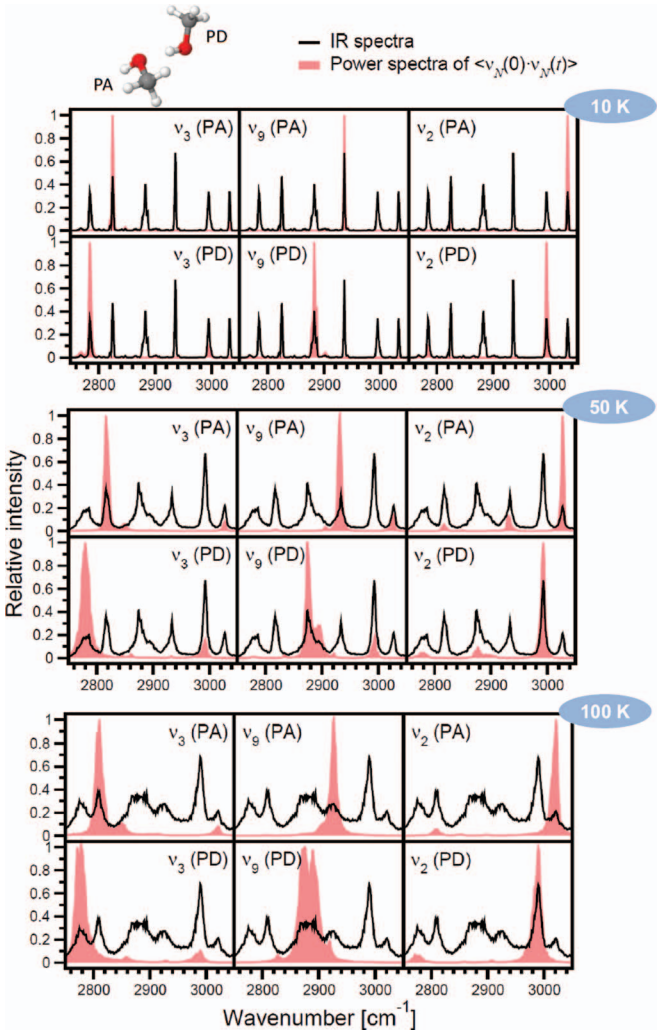

FIG. 8. Assignment of bands in the simulated FT-TCF/DFTB IR spectra (black) using power spectra of $\langle \nu_N(0) \cdot \nu_N(t) \rangle$, $N = 2$, 3, 9 (red shadow background) for methanol dimer M_2 at $T = 10$ K (upper panel), $T = 50$ K (middle panel), and $T = 100$ K (lower panel).

TABLE II. Percentage contributions of symmetrized internal coordinates ν_N of methanol to the vibrational modes ν_3, ν_9, and ν_2 of PA and PD in M_2 determined from the FT-TCF/DFTB power spectra of $\langle \nu_N(0) \cdot \nu_N(t) \rangle$.

	Symmetrized internal coordinates ν_N																	
Mode[a]	ν_3 (PA)			ν_3 (PD)			ν_9 (PA)			ν_9 (PD)			ν_2 (PA)			ν_2 (PD)		
T (K)	10	50	100	10	50	100	10	50	100	10	50	100	10	50	100	10	50	100
ν_3 (PA)	91.1	82.7	79.1	2.2	6.6	9.4	0.1	1.0	1.0	0.4	6.0	4.5	8.9	4.6	6.0	0.1	0.7	0.8
ν_3 (PD)	1.4	5.4	6.9	87.5	81.8	78.3	0.0	0.5	0.4	0.2	0.9	0.7	0.0	2.7	1.1	9.4	7.4	7.1
ν_9 (PA)	0.7	1.0	1.1	0.7	1.5	1.3	98.3	87.6	81.9	0.6	5.2	6.2	0.0	1.2	1.0	0.1	3.2	2.3
ν_9 (PD)	1.2	4.5	6.3	1.6	2.9	3.5	1.4	8.2	13.3	98.7	86.6	87.2	0.2	1.3	1.6	0.2	2.3	2.4
ν_2 (PA)	5.4	4.9	5.4	0.2	0.5	0.7	0.0	0.5	0.7	0.0	0.3	0.4	90.7	85.0	82.9	0.2	2.5	4.5
ν_2 (PD)	0.3	1.5	1.2	7.9	6.8	6.8	0.1	2.2	2.8	0.0	0.9	1.0	0.1	5.1	7.5	89.9	83.8	82.9

[a]See Table III for the corresponding vibrational frequencies.

This article is copyrighted as indicated in the article. Reuse of AIP content is subject to the terms at: http://scitation.aip.org/termsconditions. Downloaded to IP: 140.113.38.11 On: Thu, 25 Dec 2014 01:20:11

TABLE III. Experimental[54] and theoretical vibrational frequencies (cm^{-1}) of methanol dimer M_2 in the C–H stretching region.

				SCC-DFTB			
		B3LYP/ANO1[a]			FT-TCF		
Mode (PA/PD)	Experiment[a]	NMA	VPT2[b]	NMA	10 K	50 K	100 K
ν_3 (PA)	2849 ± 2	3013	2940	2818	2825	2817	2810
ν_3 (PD)	2823 ± 2	2977	2814	2777	2784	2780	2778
ν_9 (PA)	2955 ± 2	3068	2935	2928	2936	2932	2928
ν_9 (PD)	2934 ± 2	3015	2876	2875	2883	2875	2870
ν_2 (PA)	3006 ± 2	3125	2997	3023	3032	3027	3022
ν_2 (PD)	2984 ± 2	3090	2957	2986	2995	2993	2990

[a]Reference 54.
[b]Second-order vibrational perturbation theory for anharmonic frequencies.[71,72]

100 K include the effect of both methyl group rotation and the flipping associated with the PA-PD identity switching of both monomers. Interestingly enough, neither of these large-amplitude motions discussed in details in Sec. III D does not manifest itself strongly in the FT-TCF/DFTB spectra. All simulations conducted in the studied range of temperatures (10 K, 50 K, and 100 K) confirm the previous assignment in Figure 1 based on harmonic B3LYP vibrational frequencies as shown in Figure 8 and are in sharp discord with the assignment based on anharmonic B3LYP/VPT2 vibrational frequencies.

D. Large amplitude motions in methanol dimer

Previous NMA simulations of the IR spectra of methanol dimer were based on the assumption that the system probes only a small subset of the full configuration space in the close vicinity of its equilibrium geometry. Clearly, for a floppy system as the methanol dimer, such an assumption can be imprecise. We have found that already at low temperatures certain large-amplitude motions of the methanol dimer are activated, conceivably leading to serious interpretational problems in the analysis of the IR bands if inappropriately treated. Large-amplitude motions present in our FT-TCF/DFTB simulations concern the rotation of both methyl groups and a flipping of the dimer leading to switching of the roles of both monomers from PA to PD and vice versa.

The first phenomenon we would like to discuss is a slow transition from the regime of libration to the regime of free rotation of the methyl groups. At lower temperatures (10 K), the available little amount of kinetic energy indeed localizes methyl groups in one of the available three minima in the potential energy surface; at higher temperatures, transition between the minima becomes possible and happens more frequently as more kinetic energy avails. We have visualized the number of such transitions as a function of temperature in Figure 9, where we show the percentile of the MD trajectories in which at least one such a transition between adjacent libration minima occurred (the left lower panel of Figure 9) and the total number of such transitions accumulated over 100 of 50 ps trajectories (the right lower panel of Figure 9). Both values increase as the temperature elevates. The transitions seem to be activated around 30 K. At 50 K, the total number of 325 transitions (117 for PA and 208 for PD) has been observed in total of 46 trajectories. At 100 K, the total number of transitions grows to 6441, distributed almost equally between both monomers. We note that for a single methanol molecule, the temperature of approximately 160 K is required in the DFTB trajectory for a free rotation of the methyl group. The upper panel of Figure 9 shows an example of a representative trajectory recorded at 50 K in which five such rotational transitions occurred. PA has experienced a counterclockwise rotation twice at 7.3 ps and 31.9 ps as well as a clockwise rotation twice at 33.1 ps and 36.3 ps. Only one clockwise rotation is observed for PD at 23.0 ps. The transitions in PA and in PD seem to be not correlated. The presented dihedral angle τ oscillation around the equilibrium values (180° and ±60°)—with a period of 0.1–0.15 ps—is large, suggesting that already at 50 K the assumption of "small vibrations" made in the NMA analysis, and consequently in the VPT2 anharmonic treatment, may be too crude.

Another large-amplitude feature important in the dynamics of a vibrating methanol dimer is the dynamic identity of both methanol monomers, which may serve either as a PD or as a PA during a given trajectory. The PA-PD switching is

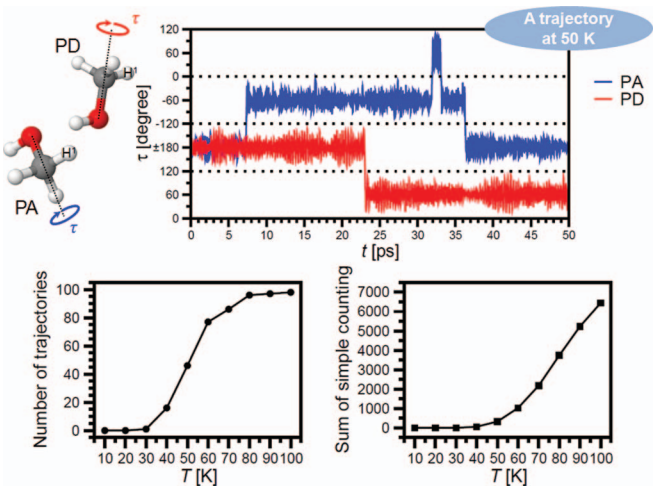

FIG. 9. Upper panel: Variation of the H^1COH dihedral angles τ in M_2 as a function of simulation time t for an exemplary trajectory. Lower panel: (Left) Number of trajectories in which methyl groups rotated between adjacent minima at least once during the simulation time as a function of temperature. (Right) Total number of rotations of methyl groups between adjacent minima during the simulation time as a function of temperature.

This article is copyrighted as indicated in the article. Reuse of AIP content is subject to the terms at: http://scitation.aip.org/termsconditions. Downloaded to IP: 140.113.38.11 On: Thu, 25 Dec 2014 01:20:11

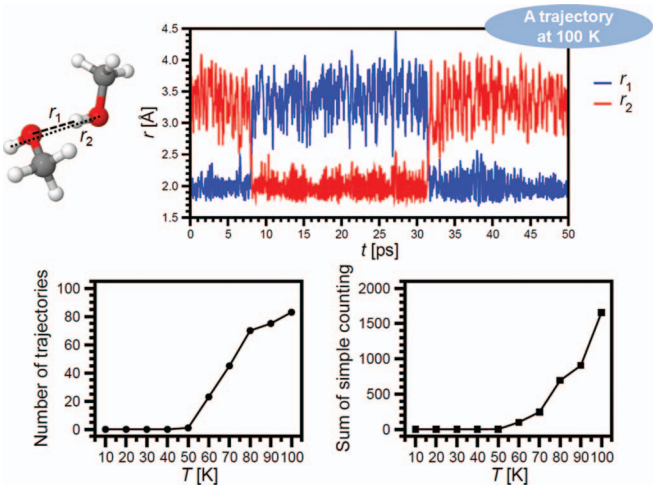

FIG. 10. Upper panel: Time evolution of the O–H intermolecular distances r_1 and r_2 (see figure for their definitions) in methanol dimer M_2 for an exemplary trajectory. Lower panel: (Left) Number of trajectories in which the PA-PD flipping occurred at least once during the simulation time as a function of temperature. (Right) Total number of the PA-PD flippings during the simulation time as a function of temperature.

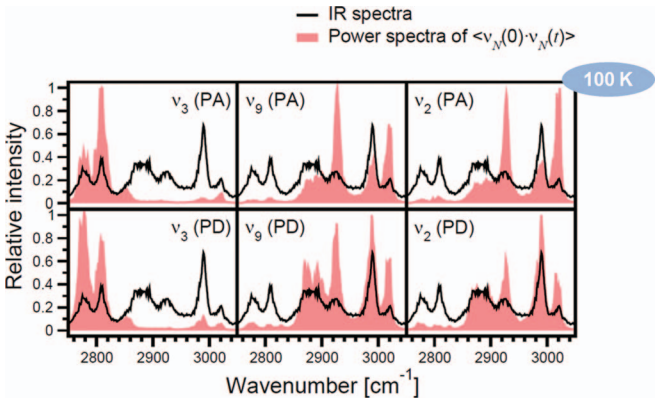

FIG. 11. Misleading assignment of the FT-TCF/DFTB IR spectra (black) using the power spectra of $\langle \nu_N(0) \cdot \nu_N(t) \rangle$, $N = 2, 3, 9$ (red shadow background) for methanol dimer M_2 at $T = 100$ K without accounting neither for the indistinguishability of the hydrogen atoms in the methyl groups rotation nor for the indistinguishability of the methanol monomers in the PA-PD flipping.

activated at approximately 50 K as can be inferred from the left lower panel of Figure 10, which shows the percentile of the MD trajectories, in which such a switch has occurred at least once. The frequency of such transitions as a function of temperature is visualized in the right lower panel of Figure 10, where we show the total number of such switches accumulated over 100 of 50 ps trajectories (the right lower panel of Figure 10); it increases fast as the temperature elevates. The upper panel of Figure 10 shows an example of a representative trajectory recorded at 100 K in which two such transitions occurred at 8.0 ps and 31.5 ps. The example of three additional high-amplitude motions, at 6.6, 26.8, and 33.0 ps, shows that the PA-PD switch not always happens despite of a sufficient amount of available kinetic energy. The PA-PD flipping happens quite often. At 100 K we have detected approximately 1700 switches between the role of PA and PD in 100 of 50 ps trajectories, which gives an average timing between switches of the order of 3 ps. This is much longer than the time needed for a single molecular vibration, which is of the order of 0.01–0.1 ps. This signifies that the clusters spend majority of time in well-defined geometrical configurations. The higher activation energy of the PA-PD flipping in comparison to the methyl group rotation is consistent with the pronounced strength of hydrogen bonding interaction energy (3.4 kcal/mol, see Figure 3), substantially larger than the rotational barrier of the methyl group (1.0 kcal/mol according to the relaxed torsion angle scan of a methanol molecule).

The large amplitude motions described here seem not to influence the shape of the FT-TCF/DFTB spectra. However, meaningful interpretation of the FT-TCF/DFTB spectra depends crucially on proper handling of large amplitude motions. If one accepts the internal coordinates of both methanols of M_2 at the time $t = 0$ as the definition of vibrational coordinates ν_i, the interpretation of IR spectra via the peak positions in FT of the $\langle \nu_N(0) \cdot \nu_N(t) \rangle$ power spectra yields very limited and misleading information. We have visualized the misleading assignment of the FT-TCF/DFTB spectra caused by the PA-PD flipping and the methyl groups rotations in Figure 11. The methyl groups rotations lead to fake strong mixing of the ν_9 and ν_2 modes and the PA-PD flipping causes fake strong mixing of bands of PA and PD. Only accounting for indistinguishability of the hydrogen atoms in the methyl group rotations and indistinguishability of the methanol monomers in the PA-PD flipping allows us to remove this unwanted fake effect causing serious interpretational difficulties. In our simulations, the indistinguishability is imposed by dynamical reordering the H atoms of the methyl groups and the monomers in the geometry files recorded during the MD trajectories prior to the projection onto the set of internal coordinates.

The large amplitude motions, discussed in this section, correspond to transitions between equivalent minima on the multidimensional potential energy surfaces. In classical description, inherent to our model, the system is allowed to roam between the equivalent minima if enough kinetic energy is available. In quantum description, the coupling between the equivalent minima happens even if there is not enough kinetic energy, manifesting itself in the tunneling splitting of the quantum levels localized in each of the equivalent minima. The two large-amplitude motions discussed here certainly result in such fine structure of vibrational levels of the dimer, which can be described symbolically as, respectively, the $(A \oplus E) \otimes (A \oplus E)$ and $A \oplus B$ tunneling splittings. It should be stressed that the tunneling effects responsible for torsional and flipping splittings of vibrational levels of the methanol dimer are completely overlooked in our intrinsically classical simulations. Finding proper way of including these quantum phenomena in the treatment based on classical trajectories remains one of the biggest challenges for the technique of simulating IR spectra employed here.

IV. CONCLUSIONS

In the present work, we have applied the SCC-DFTB method to model the vibrational IR spectra of methanol clusters. The main objective of our work is to confirm (or

This article is copyrighted as indicated in the article. Reuse of AIP content is subject to the terms at: http://scitation.aip.org/termsconditions. Downloaded to IP: 140.113.38.11 On: Thu, 25 Dec 2014 01:20:11

disprove) one of the two previously presented[54] assignments —based on harmonic B3LYP/ANO1 vibrational frequencies and anharmonic B3LYP/VPT2/ANO1 vibrational frequencies —of the IR bands in the C–H stretching region for the gas-phase methanol dimer clusters. The B3LYP/ANO1 normal mode analysis predicted small splittings between the ν_3, ν_9, and ν_2 modes of PA and PD in comparison to the analogous modes of a single methanol molecule, while B3LYP/VPT2/ANO1 predicted much larger splittings together with an interwoven pattern of the resulting modes. Two alternative formalisms based on the SCC-DFTB potential energy surfaces have been employed here for providing alternative assignments of the spectral region 2650–3150 cm^{-1}: (i) standard double-harmonic approach referred to as NMA/DFTB and (ii) Fourier transform of the dipole moment autocorrelation function approach referred to as FT-TCF/DFTB where molecular dynamics simulations have been performed at three different temperatures up to 100 K. Both approaches confirm the assignments of the C–H stretching bands based on the B3LYP/ANO1 vibrational frequencies and are in sharp discord with the assignment based on anharmonic B3LYP/VPT2/ANO1 vibrational frequencies, suggesting that some procedural faults, likely related to the breakdown of the perturbational vibrational treatment, led the B3LYP/VPT2/ANO1 calculations astray.

The IR spectra based on the FT-TCF/DFTB approach have been obtained including new, previously unaccounted for physical factors such as finite temperature, deviation of the floppy molecules from the equilibrium geometries, and large amplitude motions of the whole cluster. This goal has been accomplished by sampling a sufficient number of MD trajectories in a large portion of the potential energy surface around the equilibrium geometry. The elevation of temperature in our simulations resulted in a considerable broadening of the observed IR signals, in many situations leading to merging of the neighboring bands, particularly at higher temperatures. The broadening was not homogeneous, affecting predominantly the ν_1 and ν_9 bands and having only minute effect on ν_2. Surprisingly, the presence of large-amplitude motions—methyl group rotations and PA-PD flipping—has not introduced any new features in the spectrum. We highlight here that the detected large amplitude motions, if not appropriately treated, may lead to serious interpretational difficulties for the band identities.

The current study does not exhaust the list of interesting phenomena characteristic for methanol cluster. We believe that considerable attention, particularly from theoreticians, should be given to studying large methanol clusters, mixed water-methanol clusters, and/or protonated and deprotonated systems, close examining of the isotope effects[65] (e.g., in CH_3OD clusters), and investigation of Raman spectra by the FT-TCF approach. Elucidation of these points will enrich our knowledge on hydrogen bonded systems and will give us better techniques for interpretation of vibrational spectra.

ACKNOWLEDGMENTS

Ministry of Science and Technology of Taiwan (Grant Nos. NSC 102-2113-M-009-015-MY3 and NSC 102-2745-M-009-001-ASP) and Ministry of Education (MOE-ATU project) are acknowledged for financial support. Y.N. acknowledges financial supports by the Nagoya University Grobal COE program "Elucidation and Design of Materials and Molecular Functions" and S.I. acknowledges financial support from a Core Research for Evolutional Science and Technology (CREST) program of Japan Science and Technology Agency (JST).

[1]E. B. Wilson, J. C. Decius, and P. C. Cross, *Molecular Vibrations: The Theory of Infrared and Raman Vibrational Spectra* (Dover Publications, New York, 1980).
[2]G. Herzberg, *Molecular Spectra and Molecular Structure, Vol. II: Infrared and Raman Spectra of Polyatomic Molecules* (Krieger Publishing Company, Malabar, 1991).
[3]D. Steele, "Infrared spectroscopy: Theory," in *Handbook of Vibrational Spectroscopy, Vol. 1: Theory and Instrumentation*, edited by J. M. Chalmers and P. Griffiths (John Wiley & Sons Ltd., Chichester, 2002).
[4]G. Keresztury, "Raman spectroscopy: Theory," in *Handbook of Vibrational Spectroscopy, Vol. 1: Theory and Instrumentation*, edited by J. M. Chalmers and P. Griffiths (John Wiley & Sons Ltd., Chichester, 2002).
[5]P. Pulay and W. Mayer, Mol. Phys. **27**, 473 (1974).
[6]A. P. Scott and L. Radom, The Journal of Physical Chemistry **100**, 16502 (1996).
[7]K. K. Irikura, R. D. Johnson III, and R. N. Kacker, The Journal of Physical Chemistry A **109**, 8430 (2005).
[8]G. Rauhut and P. Pulay, The Journal of Physical Chemistry **99**, 3093 (1995).
[9]G. Rauhut and P. Pulay, J. Am. Chem. Soc. **117**, 4167 (1995).
[10]G. Rauhut and P. Pulay, The Journal of Physical Chemistry **99**, 14572 (1995).
[11]J. Baker, A. A. Jarzecki, and P. Pulay, The Journal of Physical Chemistry A **102**, 1412 (1998).
[12]J. M. Bowman, Acc. Chem. Res. **19**, 202 (1986).
[13]G. Rauhut, The Journal of Chemical Physics **121**, 9313 (2004).
[14]J. O. Jung and R. B. Gerber, The Journal of Chemical Physics **105**, 10332 (1996).
[15]D. A. McQuarrie, *Statistical Mechanics* (University Science Books, Virginia, 2000).
[16]R. G. Gordon, The Journal of Chemical Physics **43**, 1307 (1965).
[17]R. Kubo, J. Phys. Soc. Jpn. **12**, 570 (1957).
[18]M. Aida and M. Dupuis, J. Mol. Struct.: THEOCHEM **633**, 247 (2003).
[19]A. Putrino and M. Parrinello, Phys. Rev. Lett. **88**, 176401 (2002).
[20]M. Pagliai, C. Cavazzoni, G. Cardini, G. Erbacci, M. Parrinello, and V. Schettino, The Journal of Chemical Physics **128**, 224514 (2008).
[21]H. Hesske, A. Urakawa, J. VandeVondele, and A. Baiker, The Journal of Chemical Physics C **114**, 15042 (2010).
[22]J. Sauer and J. Döbler, ChemPhysChem **6**, 1706 (2005).
[23]M. Pagliai, M. Muniz-Miranda, G. Cardini, and V. Scettino, J. Mol. Struct. **993**, 151 (2011).
[24]M. Martinez, M.-P. Gaigeot, D. Borgis, and R. Vuilleumier, The Journal of Chemical Physics **125**, 144106 (2006).
[25]M.-P. Gaigeot, M. Martinez, and R. Vuilleumier, Mol. Phys. **105**, 2857 (2007).
[26]V. Schultheis, R. Reichold, B. Schropp, and P. Tavan, The Journal of Physical Chemistry B **112**, 12217 (2008).
[27]A. Miani, M. S. Helfand, and S. Raugei, J. Chem. Theory Comput. **5**, 2158 (2009).
[28]D. Porezag, T. Frauenheim, T. Köhler, G. Seifert, and R. Kaschner, Phys. Rev. B **51**, 12947 (1995).
[29]M. Elstner, D. Porezag, G. Jungnickel, J. Elsner, M. Haugk, T. Frauenheim, S. Suhai, and G. Seifert, Phys. Rev. B **58**, 7260 (1998).
[30]P. Hohenberg and W. Kohn, Phys. Rev. **136**, B864 (1964).
[31]W. Kohn and L. J. Sham, Phys. Rev. **140**, A1133 (1965).
[32]M. Meuwly, A. Müller, and S. Leutwyler, Phys. Chem. Chem. Phys. **5**, 2663 (2003).
[33]V. Zoete and M. Meuwly, The Journal of Chemical Physics **120**, 7085 (2004).
[34]A. Fouqueau and M. Meuwly, The Journal of Chemical Physics **123**, 244308 (2005).
[35]H. Yu and Q. Cui, The Journal of Chemical Physics **127**, 234504 (2007).

This article is copyrighted as indicated in the article. Reuse of AIP content is subject to the terms at: http://scitation.aip.org/termsconditions. Downloaded to IP: 140.113.38.11 On: Thu, 25 Dec 2014 01:20:11

[36]S. Kaminski, M. Gaus, P. Phatak, D. von Stetten, M. Elstner, and M. A. Mroginski, J. Chem. Theory Comput. **6**, 1240 (2010).
[37]B. Joalland, M. Rapacioli, A. Simon, C. Joblin, C. J. Marsden, and F. Spiegelman, The Journal of Physical Chemistry A **114**, 5846 (2010).
[38]A. Simon, M. Rapacioli, M. Lanza, B. Joalland, and F. Spiegelman, Phys. Chem. Chem. Phys. **13**, 3359 (2011).
[39]A. Simon, M. Rapacioli, J. Mascetti, and F. Spiegelman, Phys. Chem. Chem. Phys. **14**, 6771 (2012).
[40]H. A. Witek, S. Irle, and K. Morokuma, The Journal of Chemical Physics **121**, 5163 (2004).
[41]H. A. Witek, K. Morokuma, and A. Stradomska, The Journal of Chemical Physics **121**, 5171 (2004).
[42]H. A. Witek, K. Morokuma, and A. Stradomska, J. Theory Comput. Chem. **4**, 639 (2005).
[43]H. A. Witek, S. Irle, G. Zheng, W. A. de Jong, and K. Morokuma, The Journal of Chemical Physics **125**, 214706 (2006).
[44]E. Małolepsza, H. A. Witek, and S. Irle, The Journal of Physical Chemistry A **111**, 6649 (2007).
[45]E. Małolepsza, Y.-P. Lee, H. A. Witek, S. Irle, C.-F. Lin, and H.-M. Hsieh, Int. J. Quantum Chem. **109**, 1999 (2009).
[46]W. Li, S. Irle, and H. A. Witek, ACS Nano **4**, 4475 (2010).
[47]D. V. Kazachkin, Y. Nishimura, H. A. Witek, S. Irle, and E. Borguet, J. Am. Chem. Soc. **133**, 8191 (2011).
[48]H. A. Witek and K. Morokuma, J. Comput. Chem. **25**, 1858 (2004).
[49]E. Małolepsza, H. A. Witek, and K. Morokuma, Chem. Phys. Lett. **412**, 237 (2005).
[50]T. Häber, U. Schmitt, and M. A. Suhm, Phys. Chem. Chem. Phys. **1**, 5573 (1999).
[51]R. W. Larsen and M. A. Suhm, The Journal of Chemical Physics **125**, 154314 (2006).
[52]R. W. Larsen, P. Zielke, and M. A. Suhm, The Journal of Chemical Physics **126**, 194307 (2007).
[53]M. A. Suhm, "Hydrogen bond dynamics in alcohol clusters," in *Advances in Chemical Physics Vol. 142*, edited by S. A. Rice (John Wiley & Sons, Inc., Hoboken, 2008).
[54]H.-L. Han, C. Camacho, H. A. Witek, and Y.-P. Lee, The Journal of Chemical Physics **134**, 144309 (2011).
[55]U. Buck and F. Huisken, Chem. Rev. **100**, 3863 (2000).
[56]A. Bleiber and J. Sauer, Chem. Phys. Lett. **238**, 243 (1995).
[57]O. Mó, M. Yánez, and J. Elguero, The Journal of Chemical Physics **107**, 3592 (1997).
[58]U. Buck, J.-G. Siebers, and R. J. Wheatley, The Journal of Chemical Physics **108**, 20 (1998).
[59]F. C. Hagemeister, C. J. Gruenloh, and T. S. Zwier, The Journal of Physical Chemistry A **102**, 82 (1998).
[60]M. Masella and J. P. Flament, The Journal of Chemical Physics **108**, 7141 (1998).
[61]M. Masella and J. P. Flament, Mol. Phys. **95**, 97 (1998).
[62]G. S. Tschumper, J. M. Gonzales, and H. F. Schaefer III, The Journal of Chemical Physics **111**, 3027 (1999).
[63]M. V. Vener and J. Sauer, The Journal of Chemical Physics **114**, 2623 (2001).
[64]M. Mandado, A. M. Grana, and R. A. Mosquera, Chem. Phys. Lett. **381**, 22 (2003).
[65]R. Ludwig, ChemPhysChem **6**, 1376 (2005).
[66]S. L. Boyd and R. J. Boyd, J. Chem. Theory Comput. **3**, 54 (2007).
[67]M. M. Pires and V. F. DeTuri, J. Chem. Theory Comput. **3**, 1073 (2007).
[68]A. Mandal, M. Prakash, R. M. Kumar, R. Parthasarathi, and V. Subramanian, The Journal of Physical Chemistry A **114**, 2250 (2010).
[69]F. Billes, I. Mohammed-Ziegler, and H. Mikosch, Phys. Chem. Chem. Phys. **13**, 7760 (2011).
[70]Y.-P. Lee, Y.-J. Wu, R. M. Lees, L.-H. Xu, and J. T. Hougen, Science **311**, 365 (2006).
[71]V. Barone, The Journal of Chemical Physics **120**, 3059 (2004).
[72]V. Barone, The Journal of Chemical Physics **122**, 014108 (2005).
[73]A. D. Becke, The Journal of Chemical Physics **98**, 5648 (1993).
[74]C. Lee, W. Yang, and R. G. Parr, Phys. Rev. B **37**, 785 (1988).
[75]C. Møller and M. S. Plesset, Phys. Rev. **46**, 618 (1934).
[76]R. Krishnan, J. S. Binkley, R. Seeger, and J. A. Pople, The Journal of Chemical Physics **72**, 650 (1980).
[77]T. Clark, J. Chandrasekhar, G. W. Spitznagel, and P. v. R. Schleyer, J. Comput. Chem. **4**, 294 (1983).
[78]M. J. Frisch, G. W. Trucks, H. B. Schlegel *et al.*, Gaussian 09, Revision A.02, Gaussian, Inc., Wallingford, CT, 2009.
[79]S. F. Boys and F. Bernardi, Mol. Phys. **19**, 553 (1970).
[80]A. D. Becke, Phys. Rev. A **38**, 3098 (1988).
[81]H. J. C. Berendsen, J. P. M. Postma, W. F. van Gunsteren, A. DiNola, and J. R. Haak, The Journal of Chemical Physics **81**, 3684 (1984).
[82]J. W. Ponder and F. M. Richards, J. Comput. Chem. **8**, 1016 (1987).
[83]P. Ren and J. W. Ponder, The Journal of Physical Chemistry B **107**, 5933 (2003).
[84]D. Beeman, J. Comput. Phys. **20**, 130 (1976).
[85]B. R. Brooks, Algorithms for Molecular Dynamics at Constant Temperature and Pressure, DCRT Report, NIH, 1988.
[86]M. P. Allen and D. J. Tildesley, *Computer Simulation of Liquids* (Oxford University Press, New York, 1989).
[87]M. Frigo and S. G. Johnson, Proc. IEEE **93**, 216 (2005).
[88]S. Karthikeyan, J. N. Singh, M. Park, R. Kumar, and K. S. Kim, The Journal of Chemical Physics **128**, 244304 (2008).
[89]S. Xu, S. Irle, D. G. Musaev, and M. C. Lin, The Journal of Physical Chemistry A **109**, 9563 (2005).
[90]C. S. Lin, R. Q. Zhang, S. T. Lee, M. Elstner, T. Frauenheim, and L. J. Wan, The Journal of Physical Chemistry B **109**, 14183 (2005).
[91]M. Elstner, P. Hobza, T. Frauenheim, S. Suhai, and E. Kaxiras, The Journal of Chemical Physics **114**, 5149 (2001).
[92]M. Elstner, Theor. Chem. Acc. **116**, 316 (2006).
[93]S. Kristyán and P. Pulay, Chem. Phys. Lett. **229**, 175 (1994).
[94]J. M. Pérez-Jordá and A. D. Becke, Chem. Phys. Lett. **233**, 134 (1995).
[95]K. N. Rankin and R. J. Boyd, J. Comput. Chem. **22**, 1590 (2001).
[96]B. Santra, A. Michaelides, and M. Scheffler, J. Chem. Phys **127**, 184104 (2007).
[97]L. Rao, H. Ke, G. Fu, X. Xu, and Y. Yan, J. Chem. Theory Comput. **5**, 86 (2009).
[98]M. Elstner, T. Frauenheim, E. Kaxiras, G. Seifert, and S. Suhai, Phys. Status Solidi B **217**, 357 (2000).
[99]W.-G. Han, M. Elstner, K. J. Jalkanen, T. Frauenheim, and S. Suhai, Int. J. Quantum Chem. **78**, 459 (2000).
[100]H. Hu, Z. Lu, M. Elstner, J. Hermans, and W. Yang, The Journal of Physical Chemistry A **111**, 5685 (2007).
[101]Y. Yang, H. Yu, D. York, Q. Cui, and M. Elstner, The Journal of Physical Chemistry A **111**, 10861 (2007).
[102]P. Goyal, M. Elstner, and Q. Cui, The Journal of Physical Chemistry B **115**, 6790 (2011).
[103]M. Elstner, The Journal of Physical Chemistry A **111**, 5614 (2007).
[104]M. Gaus, Q. Cui, and M. Elstner, J. Chem. Theory Comput. **7**, 931 (2011).
[105]M. Nonella, G. Mathias, and P. Tavan, The Journal of Physical Chemistry A **107**, 8638 (2003).
[106]M. Klähn, G. Mathias, C. Kötting, M. Nonella, J. Schlitter, K. Gerwert, and P. Tavan, The Journal of Physical Chemistry A **108**, 6186 (2004).
[107]M. Schmitz and P. Tavan, The Journal of Chemical Physics **121**, 12247 (2004).
[108]G. Babitzki, G. Mathias, and P. Tavan, The Journal of Physical Chemistry B **113**, 10496 (2009).
[109]M. Schmitz and P. Tavan, The Journal of Chemical Physics **121**, 12233 (2004).
[110]R. A. Wheeler, H. Dong, and S. E. Boesch, ChemPhysChem **4**, 382 (2003).
[111]R. A. Wheeler and H. Dong, ChemPhysChem **4**, 1227 (2003).
[112]G. Mathias and M. D. Baer, J. Chem. Theory Comput. **7**, 2028 (2011).
[113]A. Miani, V. Hänninen, M. Horn, and L. Halonen, Mol. Phys. **98**, 1737 (2000).
[114]Y.-C. Sun, H. Gai, and G. A. Voth, Chem. Phys. **200**, 357 (1995).
[115]T. A. Beu, J. Onoe, and K. Takeuchi, Eur. Phys. J. D **10**, 391 (2000).
[116]T. A. Beu, J. Onoe, and K. Takeuchi, Eur. Phys. J. D **17**, 205 (2001).
[117]S. G. Estácio and B. J. Costa Cabral, Chem. Phys. Lett. **456**, 170 (2008).
[118]J. Kwiendacz, M. Boczar, and M. J. Wójcik, Chem. Phys. Lett. **501**, 623 (2011).
[119]A. Kovács, V. Izvekov, G. Keresztury, and G. Pongor, Chem. Phys. **238**, 231 (1998).
[120]K. Dobrosz-Teperek, J. C. Dobrowolski, R. Kołos, W. Lewandowski, and A. P. Mazurek, J. Mol. Struct. **563–564**, 395 (2001).
[121]M. H. Jamróz and J. C. Dobrowolski, J. Mol. Struct. **565–566**, 475 (2001).
[122]A. A. Popov, A. A. Goryunkov, I. V. Goldt, I. E. Kareev, I. V. Kuvychko, W.-D. Hunnius, K. Seppelt, S. H. Strauss, and O. V. Boltalina, The Journal of Physical Chemistry A **108**, 11449 (2004).
[123]V. Krishnakumar and R. Ramasamy, Spectrochim. Acta A **61**, 3112 (2005).
[124]V. Krishnakumar and R. Ramasamy, Spectrochim. Acta A **66**, 503 (2007).

This article is copyrighted as indicated in the article. Reuse of AIP content is subject to the terms at: http://scitation.aip.org/termsconditions. Downloaded to IP: 140.113.38.11 On: Thu, 25 Dec 2014 01:20:11